

# Atomic Structure of Small and Intermediate-Size Silver Nanoclusters

Ali M. Angulo and Cecilia Noguez\*

Instituto de Física, Universidad Nacional Autónoma de México, Apartado Postal 20-364, México D.F. 01000

Received: February 21, 2008; Revised Manuscript Received: April 8, 2008

Molecular dynamic simulations were performed to study the morphology and binding energy of the most stable isomers of silver clusters with diameters of less than 2 nm. A 5-fold symmetry was found in most cases, and a novel morphology for the clusters of 39 and 116 silver atoms was identified. This morphology can be understood in terms of decahedral and icosahedral geometries, which are intercalated, as we explain in detail. These kind of structures have been observed for gold and now are predicted for small and intermediate silver nanoparticles.

## 1. Introduction

Nanosized metal particles exhibit a wide variety of physical properties that can be tailored by altering the particle size, morphology, and composition. Knowledge of these parameters and their relationships is relevant for the systematic synthesis of nanoparticles with uniform and reliable properties. Within this context, atomic simulations play a major role in the explanation and prediction of novel nanostructures, which are complementary ingredients for experimentalists. Small metallic nanoparticles show icosahedral, decahedral, truncated octahedral, and amorphous morphologies, in contrast to macroscopic crystals, for which the face-centered cubic (fcc) atomic arrangement is predominant. Some general trends have been found, where icosahedra are favored at small sizes, decahedra at intermediate sizes, and truncated octahedra at large sizes.<sup>1</sup> The motif crossover depends on size; for example, for Ag, the icosahedral interval is rather large, and it is followed by a very wide decahedral window. Icosahedra are better for small clusters from the energetic point of view, but decahedra have less internal strain and become more favorable than icosahedra at increasing sizes.

Numerical simulations have been extremely useful in explaining the structures of silver clusters in terms of energy, thermodynamics, and kinetics<sup>1–5</sup> and provide a basis for understanding experimental observations.<sup>6–8</sup> Other structures such as truncated icosahedra<sup>9</sup> and double icosahedra<sup>10</sup> have been observed experimentally, as well as other 5-fold-symmetric nanoparticles.<sup>11</sup> However, few theoretical works have been performed to explain these morphologies.<sup>11–18</sup>

In this work, we study small and intermediate-size silver clusters. In section 2, we describe the method employed to study clusters of different sizes. In section 3, we analyze optimized structures of clusters of different sizes and compare these structures with previous results to validate the methodology used here. In section 4, we identify a novel structure for clusters with 39 and 116 silver atoms. This structure can be understood as the intercalation of an icosahedron and a decahedron. To study the reliability of these structures, we explored the surface potential at those sizes, looking for the frequency of occurrence of low-energy isomers. Then, we describe the morphology of these structures in detail. Finally, in section 5, we present our conclusions.

## 2. Methodology

To explore the atomic structure of silver clusters, we employed a simulated annealing algorithm. Here, we briefly explain the potential used in the simulation, the numerical details, and the criteria employed to find the low-energy isomers for each Ag<sub>*n*</sub> cluster, where *n* is the number of atoms.

**2.1. The Potential.** A semiempirical potential for the metal bonds, based on the second-moment approximation of the electron density states in the tight-binding Hamiltonian, was employed to reproduce the force between atoms.<sup>19</sup> The potential, known as the Gupta model, contains an attractive term that corresponds to an effective band due to the large d-band density of states. It also contains a short-range repulsive pair-potential term. Thus, the potential is usually expressed as

$$V_j = A \sum_{i(\neq j)=1}^n e^{-p(r_{ij}/r_0-1)} - \xi \left( \sum_{i(\neq j)=1}^n e^{-2q(r_{ij}/r_0-1)} \right)^{1/2} \quad (1)$$

where parameters *p* and *q* depend on the atom type and can be obtained by fitting to the bulk equilibrium distance and elastic constants. The parameters *A* and  $\xi$  can be obtained by minimizing the fcc bulk cohesive energy. Here,  $r_{ij} = |\vec{r}_i - \vec{r}_j|$  is the distance between atoms *i* and *j*, and *r*<sub>0</sub> is the first-neighbor distance in an fcc silver crystal. For our study, we employed the parameters reported in ref 20, where *p* = 10.928 and *q* = 3.139 are dimensionless constants, *A* = 0.1028 eV, and  $\xi$  = 1.178 eV.

**2.2. Numerical Details.** To perform the dynamics simulations, we took into account the characteristic time *t*<sub>0</sub>, which yields the oscillation period of a dimer near equilibrium. This characteristic time was found to be the same for dimers as well as larger clusters formed by up to hundreds of atoms.<sup>21</sup> In our case, the characteristic time for silver is  $t_0 \equiv r_0(m_0/E_0)^{1/2} = 0.4686$  ps, where *m*<sub>0</sub> is the atomic mass and *E*<sub>0</sub> = 2 $\xi$  for the bulk. Here, the oscillations near equilibrium were simulated with a time interval of  $\Delta t = 0.01t_0$ , and the dynamics was performed using the Verlet algorithm within the Gupta potential.

The simulated annealing consisted of heating an fcc structure of *n* silver atoms to a given temperature *T*<sub>h</sub>, just before the atoms started to be evaporated. At the temperature *T*<sub>h</sub>, we relaxed the structure in order to find different initial configurations. Then, we allowed these initial structures to cool slowly, to remove internal stresses as much as possible, until the kinetic energy was close to zero, at a temperature denoted as *T*<sub>c</sub>. Then, we

\* Corresponding author. E-mail: cecilia@fisica.unam.mx.

**TABLE 1: Parameters Employed in the Simulated Annealing for  $\text{Ag}_n$  Clusters**

$n$	$\alpha_h$	$N_h$	$T_h$ (K)	$\alpha_c$	$N_c$	$T_c$ (K)
7	1.1	4	1046.70	0.98	902	0.00
12	1.1	9	1264.43	0.96	3000	0.00
13	1.3	20	961.07	0.95	320	0.00
14	1.2	8	1181.44	0.98	447	0.35
16	1.2	8	931.24	0.98	3000	0.00
20	1.2	7	1059.39	0.98	2284	0.00
21	1.2	8	1347.43	0.98	592	0.03
23	1.2	7	998.47	0.98	3000	0.00
32	1.2	13	978.23	0.98	1922	0.00
37	1.2	15	831.26	0.98	975	0.00
38	1.2	12	1151.12	0.99	2357	0.00
39	1.2	11	1181.19	0.98	2110	0.00
48	1.2	11	783.15	0.98	713	0.00
54	1.3	11	1339.11	0.98	2695	0.00
55	1.3	24	927.04	0.98	1087	0.00
62	1.2	12	1069.31	0.98	683	0.01
64	1.2	10	794.54	0.98	969	0.00
72	1.2	15	1125.84	0.98	588	0.02
75	1.1	13	614.22	0.98	427	0.22
94	1.2	14	1081.93	0.98	417	0.63
101	1.2	14	1021.83	0.98	469	0.19
108	1.2	17	1023.95	0.98	1127	0.00
116	1.2	14	991.04	0.98	688	0.00
144	1.2	18	928.39	0.98	277	8.13
147	1.1	31	948.50	0.95	594	0.00
160	1.2	17	1247.35	0.98	342	2.53
180	1.2	18	949.27	0.98	666	0.01
192	1.2	18	747.55	0.98	293	3.98
256	1.2	22	1062.59	0.98	565	0.03
260	1.2	19	946.35	0.98	300	5.18
300	1.2	18	669.81	0.98	385	0.57
309	1.3	17	871.49	0.98	599	0.01
320	1.2	22	873.55	0.98	400	0.74
561	1.2	12	1029.08	0.98	344	243.65

relaxed the structure to search for the lowest-energy isomer at the surface potential. To heat the structure, we multiplied the velocity of each atom by a factor  $\alpha_h > 1$ , such that kinetic energy was added to the system. To cool the structure, we multiplied the velocities by a factor  $\alpha = \alpha_c < 1$ , such that energy was being absorbed from the system. When  $\alpha = 1$ , the system was being relaxed according to the potential surface at constant kinetic energy.

At each stage, heating, cooling, or relaxing, we allowed the system to evolve for  $N_{h/c/r}$  steps, giving a total time for each stage of  $t_s = N_{h/c} \times \Delta t$ . In our simulations, during the cooling process, we typically performed  $N_c \approx 50 \times 10^4$  steps, so that the total simulation times were on the order of nanoseconds. In the search for the low-energy isomers, we performed a general exploration of the atomic structure of different size clusters, choosing  $n$  in the vicinity of the magic numbers of icosahedral clusters. After completing the simulations, we compared our results with other calculations and experiments, where the cohesive energy and shape of each structure were studied.

### 3. Optimized Structures

In Table 1, we list the different parameters of our simulation of silver clusters with  $7 \leq n \leq 561$  atoms. The heating temperatures,  $T_h$ , were of the order of  $10^3$  K, and the kinetic energy was removed in almost all cases, i.e.,  $T_c \approx 0$ . Using the parameters in Table 1, we found mostly 5-fold-symmetric clusters (i.e., icosahedra) and decahedral shapes. For the magic numbers  $n = 13, 55, 147, 309$ , and 561 atoms, we found regular icosahedra, as expected, even when the kinetic energy of the

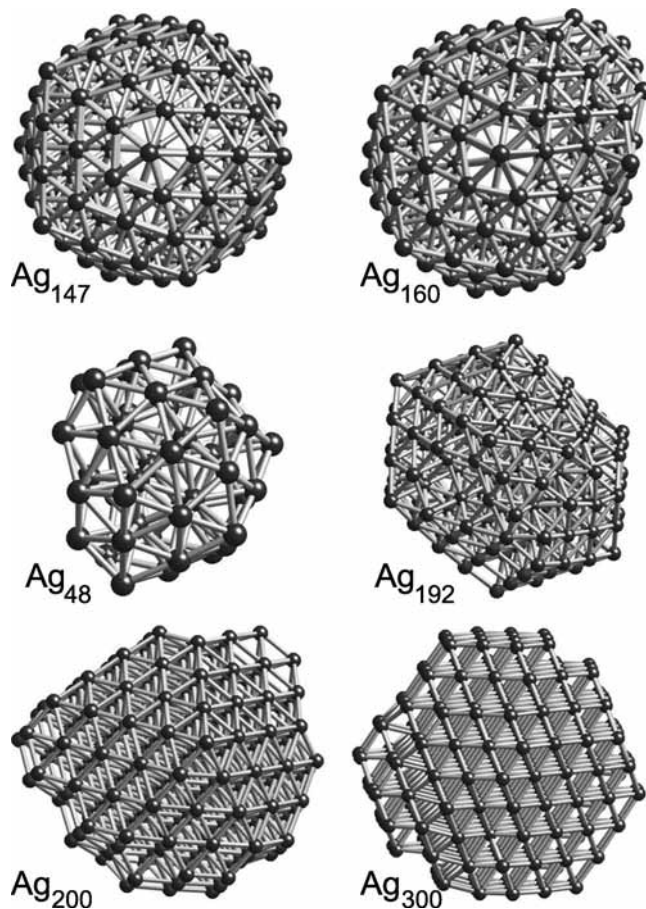


**Figure 1.** Geometries of the optimized structures, showing the main structural motifs: icosahedron  $\text{Ag}_{147}$ , icosahedron plus aggregate  $\text{Ag}_{160}$ , incomplete icosahedron  $\text{Ag}_{48}$ , overlapping icosahedra  $\text{Ag}_{192}$ , decahedron  $\text{Ag}_{200}$ , and truncated octahedron  $\text{Ag}_{300}$ .

largest cluster with  $n = 561$  atoms was not completely removed. For the clusters with  $n$  close to a magic number, i.e.,  $n = 16, 62, 160$ , and 320 atoms, we found regular icosahedra plus an aggregate of atoms that partly covered the shell of the next regular icosahedron. In addition, we found incomplete icosahedra for  $n = 12, 48, 52$ , and 144, which are also close to the magic numbers of icosahedra. We also found the typical structure of two overlapping icosahedra for  $n = 20, 21, 23, 180$ , and 192 atoms.

For the clusters with  $n = 7, 37, 72, 101, 200$ , and 260 atoms, we found regular and Marks decahedral clusters, some of which were incomplete, because the numbers of atoms are not the magic numbers for decahedral structures. Among other isomers, we found a truncated octahedron for  $n = 38, 256$ , and 300 atoms. These geometries are cubic and correspond to the fcc structure found in bulk crystals. In Figure 1, we show some examples of the structural motifs found for the optimized structures. We also found an interesting morphology family that has not been reported previously for silver clusters. This family correspond to  $\text{Ag}_n$  with  $n = 39$  and 116, in which a combination of decahedral and icosahedral structures was obtained. In the next section, we explain these structures in detail.

We also calculated the cohesive energy per atom,  $E_c/n$ , for the  $\text{Ag}_n$  clusters in Table 1, given by<sup>22</sup>

$$E_c/n = A + Bn^{-1/3} + Cn^{-2/3} + Dn^{-1} \quad (2)$$

where the constant  $A$  corresponds to the cohesive energy per atom in the bulk and the terms corresponding to constants  $B$ ,

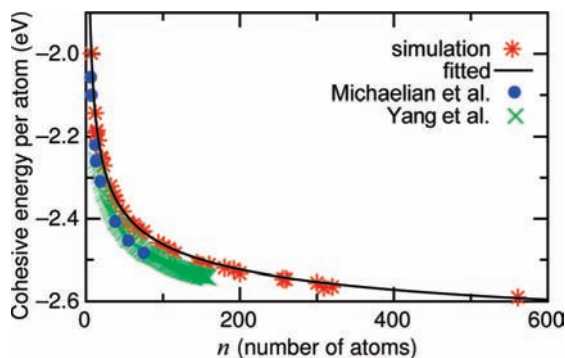


**Figure 2.** Cohesive energy per atom as a function of  $n$ : (\*) our simulation, (—) fitted curve from eq 2, (●) simulation of ref 12, and (×) simulation of ref 13.

**TABLE 2: Frequency of Occurrence of  $\text{Ag}^{37}$  Isomers of Low Energy**

$\alpha_c$	isomer 1 (-86.82 eV)	isomer 2 (-86.76 eV)	isomer 3 (-86.73 eV)	other (>-86.72 eV)
0.99	1	0	7	2
0.98	1	1	5	3
0.97	0	0	6	5

$C$ , and  $D$  represent the contributions from the atoms in the faces, edges, and vertices, respectively. Therefore, as  $n$  increases,  $A$  should approach the value of the fcc cohesive energy in a crystal. In Figure 2, we show the results of our simulations (\*) and the fitted curve (solid line) with the fitted values  $A = -2.77$  eV,  $B = 1.56$  eV,  $C = -0.92$  eV, and  $D = 1.44$  eV. Note that the cohesive energy per atom in a bulk fcc Ag crystal is  $-2.96$  eV. The deviations of  $A$  from the bulk value might be due to the small number of atoms  $n$  considered in our simulations. In Figure 2, we also show the cohesive energy per atom of previous calculations from refs 12 and 13. In both of those simulations, the Gupta model was also employed, although the parameters were slightly different. This is the reason for the apparent vertical displacement, but the curves show the same behavior as a function of  $n$ ; in any case, both sets of results, those in refs 12 and 13 and ours, were fitted to the bulk. Experimentally, 5-fold and icosahedral symmetry have been found on silver cluster cations for sizes  $n = 36$ – $46$  and  $55$  at  $120$  K.<sup>11</sup> Specifically, global order having icosahedral symmetry was found for the magic number  $n = 55$ , and a local order having 5-fold symmetry was found for  $n = 36$ – $39$  and  $43$ .

We found very good agreement between our calculations and previous theoretical simulations, where the global minima were searched using genetic algorithms, the dynamic lattice searching method, and density functional theory (DFT) molecular dynamics.<sup>11–15</sup> The first two methodologies can explore thousands of different geometries, in contrast to our simulated annealing, where only 30 initial configurations were explored. We also found very good agreement with DFT calculations of the structural stability of small silver clusters up to  $n = 23$  atoms.<sup>15</sup> Thus, it is remarkable that we found the same geometries for the low-energy isomers. For instance, we found fcc and amorphous structures for  $\text{Ag}_{38}$ ;<sup>12</sup> a decahedral structure for  $\text{Ag}_{116}$ ,<sup>13</sup> as discussed in detail in the next section; and interpenetrating icosahedra for  $n = 20, 21,$  and  $23$  atoms.<sup>15</sup> Thus, our methodology and parameters were able to reproduce well the results of previous simulations of small and medium-size clusters that used more accurate methods,<sup>11–15</sup> and we analyze in detail the novel structures found for  $n = 39$  and  $116$  atoms in the next section.

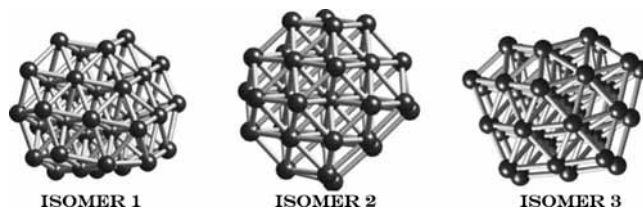


**Figure 3.** Low-energy  $\text{Ag}_{37}$  isomers.



**Figure 4.** Low-energy  $\text{Ag}_{38}$  isomers.

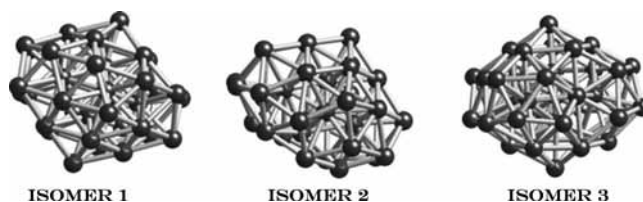


**Figure 5.** Low-energy  $\text{Ag}_{39}$  isomers.

#### 4. $\text{Ag}_{39}$ and $\text{Ag}_{116}$ Clusters

As already mentioned, we found interesting structures for  $\text{Ag}_{39}$  and  $\text{Ag}_{116}$  that have not been studied in detail before for silver clusters. To perform a better search for the low-energy structures, we performed a second set of simulations to locate isomers with  $n = 37, 38, 39,$  and  $116$  atoms. Because the surface potentials of the clusters are complex and the number of local minima increases with size, we adapted a second strategy to explore such minima. For each of these clusters with a given value of  $n$ , the initial structure was heated until a liquid structure near the gas state was obtained. Then, the system was relaxed at constant temperature to generate 30 different liquid structures to be used in subsequent annealing simulations. We cooled the structures using three different cooling parameters  $\alpha_c = 0.97, 0.98,$  and  $0.99$ , to avoid the attraction of local minima as much as possible. Finally, we analyzed the structures that appear more frequently by identifying the lowest-energy isomers.

**4.1.  $\text{Ag}_n$  with  $n = 37$ – $39$ .** Independently of  $\alpha_c$ , we found a  $\text{Ag}_{37}$  isomer of low energy that appeared 60% of the time, as shown in Table 2, which we denoted as isomer 3. This is not the isomer of lowest energy, but it is the most frequent structure for any value of  $\alpha_c$ . Isomer 3 has an incomplete decahedral structure, as shown in Figure 3. On the other hand, isomers 1 and 2 have lower energies, but they appeared only twice and once, respectively, in 30 different relaxed structures. Isomer 1 is a low-symmetry structure and has only a specular plane of symmetry, in agreement with other calculations.<sup>13</sup> Isomer 2 is an incomplete truncated octahedron, in which only one atom is missing in comparison with the  $\text{Ag}_{38}$  fcc structure.

The  $\text{Ag}_{38}$  clusters exhibit four isomers; the one with the lowest energy is a truncated octahedron, denoted as isomer 1, as shown in Figure 4. Recall that  $n = 38$  is a magic number for the fcc structures; however, the frequency of this isomer is only 10%, as shown in Table 3. The second low-energy isomer is a truncated icosahedron, similar to that found for  $\text{Ag}_{39}$ . There is experimental evidence for the observation of this isomer, which



**TABLE 3: Frequency of Occurrence of Ag<sub>38</sub> Isomers of Low Energy**

$\alpha_c$	isomer 1 (-89.52 eV)	isomer 2 (-89.35 eV)	isomer 3 (-89.25 eV)	isomer 4 (-89.20 eV)	others (> -89.20 eV)
0.99	1	1	5	2	2
0.98	2	0	1	4	2
0.97	0	0	2	8	0

**TABLE 4: Frequency of Occurrence of Ag<sub>39</sub> Isomers of Low Energy**

$\alpha_c$	isomer 1 (-91.91 eV)	isomer 2 (-91.83 eV)	isomer 3 (-91.75 eV)	others (> -91.69 eV)
0.99	4	3	1	2
0.98	3	0	1	3
0.97	7	0	2	1

**TABLE 5: Frequency of Occurrence of Ag<sub>116</sub> Isomers of Low Energy**

$\alpha_c$	isomer 1 (-288.25 eV)	isomer 2 (-288.10 eV)	isomer 3 (-288.04 eV)	others (> -287.83 eV)
0.99	3	5	0	2
0.98	1	7	0	2
0.97	0	1	1	8

could be the most stable for cationic clusters.<sup>16</sup> This structure was also found in another study that employed different empirical potentials.<sup>17</sup> Isomer 4 is the most frequent structure (46%), followed by isomer 3 at 26%. These isomers along with isomer 1 have been reported previously for this cluster size.<sup>12</sup> Isomer 4 has the lowest symmetry, although a 5-fold local order was found, as has been observed experimentally.<sup>11</sup>

For the Ag<sub>39</sub> cluster, the isomer of lowest energy is also the most frequent one, with an occurrence of 47%, as shown in Table 4. Isomer 1 is a truncated icosahedron, and isomers 2 and 3 are similar structures in which only one or two atoms are located in different positions at the surface, as shown in Figure 5. This truncated icosahedron has 5-fold symmetry, and its morphology resembles a structure in which a Ag<sub>13</sub> icosahedron and a Ag<sub>23</sub> decahedron overlap, sharing 7 atoms, with 10 more atoms added to complete the structure. The same morphology was found for other sizes, as seen for  $n = 38$ , for which there is also experimental evidence of its existence.<sup>16</sup> This structure was also found for  $n = 116$  as described in the next section.

In summary, it was found that the most frequent low-energy structures for Ag<sub>*n*</sub> with  $n = 37-39$  were not the same. We found a decahedron, a low-symmetry structure, and a truncated icosahedron as the most stable isomers for  $n = 37-39$ , respectively. This means that there is no particular trend in morphology at this cluster size. We also found that the global minimum does not correspond to the most frequent stable low-energy isomer. This is an effect of the form of the surface potential, which is complex and includes a number of local minima that increases rapidly with the cluster size. These minima can be very close in energy to the global minimum, so that the isomers are essentially degenerate. These minima have basins of different widths, such that the probability of reaching each minimum is given by the width. For example, the energy difference between isomers 1 and 4 of Ag<sub>38</sub> is less than 0.009 eV per atom; however, the basin of isomer 4 must be wider, as this isomer is found more frequently.

**4.2. Ag<sub>116</sub> Cluster.** The isomer of lowest energy for Ag<sub>116</sub> appears 13% of the time. It exhibits a Marks decahedron structure with 15 additional atoms located at the outer shell, as seen in Figure 6. Depending on where these 15 extra atoms are located, the energy of isomer 1 varies slightly from -288.29

to -288.22 eV, as shown in Table 5. One should recall that, as the number of atoms increases, the surface potential becomes increasingly complex, such that local minima can be degenerate. These decahedra were also found in previous calculations.<sup>13</sup> Isomer 2 is a truncated icosahedron, which is the most frequent structure for this size, with a frequency of occurrence of 43%. Notice that the average energy difference between isomers 2 and 1 is very small, at less than  $\sim 0.002$  eV per atom, but the structures are completely different. On the other hand, isomer 3 is also a Marks decahedron, but again with a low frequency of occurrence. The other isomers with higher energy account for 40%, and they are Marks decahedra (four clusters) and truncated icosahedra (eight clusters). For the Ag<sub>115</sub> cluster, we found similar results, even when using only 10 initial configurations. Therefore, at this size, we found a trend of the morphology, in contrast to our finding at smaller sizes.

We performed additional DFT optimizations, within the generalized gradient approximation,<sup>23</sup> of the low-energy isomers reported in this section. We found that, for the isomers with  $n = 38$ , the fcc structure assigned to isomer 1 was still the structure of lowest energy. The truncated icosahedron has an energy difference of only -0.43 eV, and isomer 3 has a difference of -0.97 eV. For the isomers with  $n = 39$ , we observed the same trend, with isomer 1 being the most stable and isomers 2 and 3 having energy differences of -0.41 and -0.66 eV, respectively. For  $n = 116$ , the results changed slightly: isomer 2, the truncated icosahedron, was the one of lowest energy, with difference of -0.5 eV for isomer 1 and -0.98 eV for isomer 3. Thus, using DFT, we corroborated our findings using the Gupta potential, according to which the truncated icosahedron is a stable isomer for silver clusters with  $n = 38, 39$ , and 116 atoms. In the case of  $n = 38$ , there is also experimental evidence for the existence of this structure.<sup>16</sup>

**4.3. Morphology of the Truncated Icosahedra.** The truncated icosahedra found here can be constructed by the combination of a regular icosahedron and a regular decahedron. In Figure 7, we show top, bottom, and side views of these structures for Ag<sub>39</sub> and Ag<sub>116</sub>. Both nanoclusters have 5-fold symmetry, but the top view shows a decagon (left-hand side of Figure 7), whereas the bottom view shows a pentagon (right-hand side of Figure 7). The morphology has 30 faces, 10 of which are equilateral triangles, such that five of the triangles form the icosahedral shape on the top and the other five share their vertices with five rectangles that form a decagon. On the bottom, five equilateral triangles share one vertex, forming a pentagon. The side is formed by five equilateral triangles and five isosceles trapezoids.

These structures cannot be generated from icosahedra and decahedra by using simple geometrical operations such as rotations and mirror images, even when they have 5-fold symmetry. These morphologies for Ag<sub>39</sub> and Ag<sub>116</sub> can be thought of as consisting of an icosahedron and a decahedron. In Figure 8, we show the composition of the Ag<sub>116</sub> cluster, which can be explained as follows: Consider an icosahedron with 55 atoms, shown in Figure 8a, and a decahedron of 54 atoms, shown in Figure 8b. Then, we intercalate the two structures, as shown in Figure 8c, in such a way that they share 23 atoms.

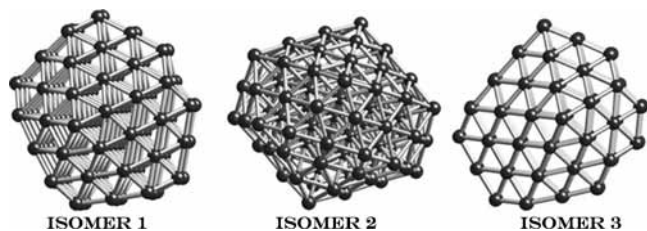


Figure 6. Low-energy  $\text{Ag}_{116}$  isomers.

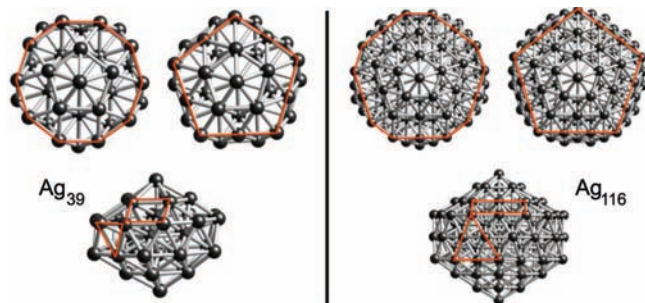


Figure 7. Top, bottom, and side views of  $\text{Ag}_{39}$  and  $\text{Ag}_{116}$  truncated icosahedra.

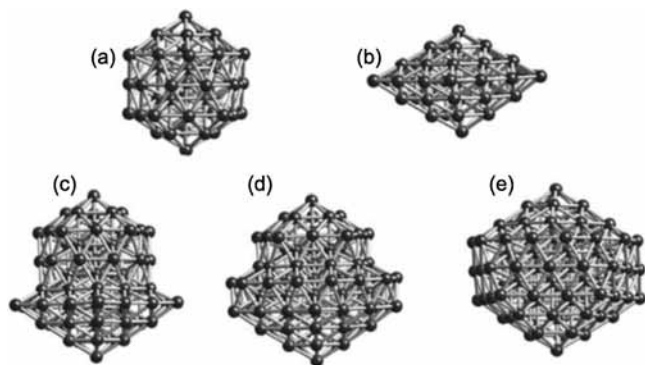


Figure 8. Atomic model of the construction of the  $\text{Ag}_{116}$  truncated icosahedron from (a) a  $\text{Ag}_{55}$  icosahedron and (b) a  $\text{Ag}_{54}$  decahedron (c) that are intercalated and share 23 atoms where (d,e) another 30 atoms are added around the icosahedron to complete the 5-fold-symmetric structure.

Then, 15 atoms are added to form a decagon around the icosahedron, as shown in Figure 8d, and finally, another 15 atoms are added at the top, also around the icosahedron, to form another decagon. The same procedure can be followed to form the  $\text{Ag}_{39}$  cluster, in which an icosahedron of 13 atoms and a decahedron of 23 atoms are intercalated by sharing 7 atoms and 10 more atoms are added around the icosahedron. This kind of hybridization for medium-size silver clusters was predicted by Baletto et al.<sup>24</sup>

These morphologies have been observed in gold nanoparticles at different sizes by using high-resolution transmission electron microscopy (HRTEM).<sup>9</sup> In that work, an extensive search for gold nanostructures was also performed using molecular dynamics, and the potential surface was explored using genetic algorithms. Also, these types of truncated icosahedra have been found to be stable for copper, palladium, and gold, using the embedded atom method,<sup>18</sup> and for sodium clusters using the Murrell–Mottram potential.<sup>25</sup>

## 5. Conclusions

We have found that 5-fold structures are preferred by small and medium-size silver clusters, with icosahedra being more

frequent at small sizes whereas decahedra are more frequent for intermediate sizes. These findings are in agreement with other theoretical results and experimental observations. We studied the low-energy isomers of silver clusters with 37–39 atoms. We found that the minimum-energy structure and the most frequent structure were not the same, because of the potential surface shape, where some global minimum basins are narrower than others, such that they are less probable even if they are deeper. At such cluster sizes, we did not find a specific trend in the structure, although the more frequent isomers had 5-fold symmetry. We found a novel morphology for the silver cluster of 39 atoms that was also observed for the cluster of 116 atoms. Such a structure has been observed experimentally in gold clusters and predicted for palladium and sodium; however, this is the first time it was obtained for silver. There is experimental evidence that this morphology exists for clusters of 38 atoms, along with other theoretical predictions that support our findings. We describe in detail the structure of this truncated icosahedron, which is built from an intercalated icosahedron and decahedron. This structure is different from other truncated icosahedra, which are formed from two icosahedra.

**Acknowledgment.** We acknowledge fruitful discussions with Ignacio L. Garzón. We also thank Juan A. Reyes-Nava and Ignacio L. Garzón for making available the molecular dynamics code. Partial financial support from CONACyT (Grant 48521) and DGAPA-UNAM (Grant IN106408) is acknowledged. Computer resources from DGSCA-UNAM are also acknowledged.

## References and Notes

- Baletto, F.; Ferrando, R.; Fortunelli, A.; Montalenti, F.; Mottet, C. *J. Chem. Phys.* **2002**, *116*, 3856.
- Tian, Z.-M.; Tian, Y.; Wei, W.-M.; He, T.-J.; Chen, D.-M.; Liu, F.-C. *Chem. Phys. Lett.* **2006**, *420*, 550.
- Matulis, V. E.; Ivashkevich, O. A.; Gurin, V. S. *J. Mol. Struct.* **2003**, *664*, 291.
- Fournier, R. *J. Chem. Phys.* **2001**, *115*, 2165.
- Erkoç, Ş.; Yılmaz, T. *Phys. E* **1999**, *5*, 1.
- Hall, B. D.; Flüeli, M.; Monot, R.; Borel, J. P. *Phys. Rev. B* **1991**, *43*, 3906.
- Reinhard, D.; Hall, B. D.; Ugarte, D.; Monot, R. *Phys. Rev. B* **1997**, *55*, 7868.
- Weis, P.; Bierweiler, T.; Gilb, S.; Kappes, M. M. *Chem. Phys. Lett.* **2002**, *355*, 355.
- Ascencio, J. A.; Pérez, M.; José-Yacamán, M. *Surf. Sci.* **2000**, *447*, 73.
- Nepigko, S. A.; Hofmeister, H.; Sack-Kongehl, H.; Schlögl, R. *J. Cryst. Growth* **2000**, *213*, 129.
- Xing, X.; Danell, R. M.; Garzón, I. L.; Michaelian, K.; Blom, M. N.; Burns, M. M.; Parks, J. H. *Phys. Rev. B* **2005**, *72*, 081405.
- Michaelian, K.; Rendón, N.; Garzón, I. L. *Phys. Rev. B* **1999**, *60*, 2000.
- Yang, X.; Cai, W.; Shao, X. *J. Phys. Chem. A* **2007**, *111*, 5048.
- Baletto, F.; Mottet, C.; Ferrando, R. *Phys. Rev. Lett.* **2000**, *84*, 5544.
- Pereiro, M.; Baldomir, D. *Phys. Rev. A* **2007**, *75*, 033202.
- Blom, M. N.; Schooss, D.; Stairs, J.; Kappes, M. M. *J. Chem. Phys.* **2006**, *124*, 244308.
- Alamanova, D.; Grigoryan, V. G.; Springborg, M. *J. Phys. Chem. C* **2007**, *111*, 12577.
- Rodríguez-López, J. L.; Montejano-Carrizales, J. M.; José-Yacamán, M. *Mod. Phys. Lett. B* **2006**, *20*, 725.
- Rosato, V.; Guillope, M.; Legrand, B. *Philos. Mag. A* **1989**, *50*, 321.
- Cleri, F.; Rosato, V. *Phys. Rev. B* **1993**, *48*, 22.
- Reyes-Nava, J. A. Ph.D. Thesis, Universidad Nacional Autónoma de México, México D. F., 2005.
- Balletto, F.; Ferrando, R.; Fortunelli, A.; Montalenti, F.; Mottet, C. *Rev. Mod. Phys.* **2005**, *77*, 371.
- (a) Ordejon, P.; Artacho, E.; Soler, J. M. *Phys. Rev. B* **1996**, *53*, R10441. (b) Soler, J. M.; Artacho, E.; Gale, J. D.; Garcia, A.; Junquera, J.; Ordejon, P.; Sanchez-Portal, D. *J. Phys.: Condens. Matter* **2002**, *14*, 2745.
- Baletto, F.; Mottet, C.; Ferrando, R. *Phys. Rev. B* **2001**, *63*, 155408.
- Noya, E. G.; Doye, J. P. K.; Wales, D. J.; Aguado, A. *Eur. Phys. J. D* **2007**, *57*.